Pyrochlore from weathered carbonatite at Lueshe, Zaire

F. WALL, C. T. WILLIAMS, A. R. WOOLLEY

Department of Mineralogy, Natural History Museum, Cromwell Road, London, SW7 5BD, UK

AND

M. NASRAOUI

Département de Géochimie, Ecole des Mines de St Etienne, 158, Cours Fauriel 42100, St. Etienne, France

Abstract

A detailed study of weathered pyrochlore in the laterite above carbonatite at Lueshe, NE Zaire, has been made in order to determine its chemical and textural variations. Pyrochlore in fresh carbonatite at Lueshe is close to an ideal formula of $(Ca,Na)_2Nb_2O_6(OH,F)$ (where a general formula is $A_{2-x}B_2O_6(OH,F)_{1-y} \cdot zH_2O$). The first and principal change on weathering occurs at the base of the profile and involves the leaching and partial exchange of A cations together with hydration. This change appears common to weathered pyrochlore worldwide. As a result weathered pyrochlore at Lueshe has a large apparent A cation deficiency with A totals between 0.25 and 0.59. The B cations remain stable. Abundant kalipyrochlore is unique to Lueshe and is thought to be related to the abundance of potassium feldspar in the fresh carbonatite, showing that the actual composition of weathered pyrochlore is a characteristic of a particular deposit. Weathered profiles at Lueshe are not simple trends from the least to most leached compositions. Further factors including variation in whole rock mineralogy and chemistry, and cation exchange and uptake are responsible for local concentrations of strontio-, bario- and calcium-rich, sodium-poor pyrochlore in the ore body, as well as rims of ceriopyrochlore on kalipyrochlore. The most important textural relationship in the Lueshe pyrochlore is the intimate intergrowth with crandallite in the most weathered parts of the laterite. Although pyrochlore persists throughout the weathering profile, niobium-bearing goethite is thought to represent the final product of pyrochlore breakdown.

KEYWORDS: pyrochlore, carbonatite, weathering, kalipyrochlore, Zaire.

Introduction

MINERALS of the pyrochlore subgroup are the principal economic source of niobium and are relatively abundant in many intrusive carbonatites but mined only from the carbonatite occurrences of Araxá and Catalão, Brazil, St Honoré, Canada and Lueshe, Zaire. These four operations are responsible for >90% of niobium production world-wide. Niobium is also produced from loparite which occurs in nepheline syenite of the Lovozero intrusion, Kola Peninsula, Russia, and as a by-product of some tin production. In Brazil and Zaire intense weathering of the carbonatite has produced residual soils in which the pyrochlore has been concentrated. Although it has survived the weathering process, the pyrochlore has undergone major chemical and textural changes, and it is these changes in the Lueshe pyrochlore that are the principal subject of this paper. In order to increase the efficiency of the beneficiation process, a project has been undertaken, involving over 800 electron microprobe analyses of pyrochlore, to investigate in detail the textural relationships and compositional variation of pyrochlore throughout the deposit. This paper also aims to describe and interpret the alteration processes affecting the pyrochlore and to compare these with weathering processes affecting pyrochlore from similar deposits.

The name pyrochlore describes a mineral group, subgroup, and species (Hogarth, 1977). The general formula of the group is $A_{2-m}B_2O_6(O,OH,F)_{1-n} \cdot pH_2O$. In the pyrochlore subgroup, the B site

contains Nb+Ta > 2Ti and Nb>Ta. In the pyrochlore species, the main *A* cations are Ca+Na with no other cations accounting for >20% of the *A* atoms. Other pyrochlore species include bariopyrochlore, ceriopyrochlore, kalipyrochlore and uranopyrochlore.

Geology and previous work

The Lueshe carbonatite complex is situated in the Rwindi Mountains approximately 70 km north of Lake Kivu and 40 km southwest of Lake Edward (Idi Amin), Zaire. It is situated immediately west of the western margin of the Western Branch of the East African Rift. A K-Ar determination on biotite from Lueshe sövite gives a date of 516 ± 26 Ma (Bellon and Pouclet, 1980) but this probably reflects the Pan-African thermal event, the complex having been intruded earlier. The general geology of Lueshe has been described by Maravic and Morteani (1980) and Maravic *et al.* (1989). An early description was given by Meyer (1958).

About half of the Lueshe complex comprises cancrinite syenite the rest consisting of calcite and dolomite carbonatites. The calcite carbonatites in the southern half of the complex are overlain by lateritic soils in which pyrochlore is concentrated (Fig. 1). The laterite has been extensively drilled and sampled, generally down to bedrock. It is up to 50 m thick on the higher, flatter ground but the area is deeply incised and on the steep easterly slopes of Mutoro Hill the laterite reaches its greatest thickness.

The most detailed study of the pyrochlore heretofore is that of Van Wambeke (1965) who presented analyses of both the primary and weathered pyrochlore, as well as detailed descriptions of the physical properties. He demonstrated that the weathering process led to leaching of Na, Ca and F and the enrichment of K, Sr and water with an overall depletion of the cations in the *A* sites of the pyrochlore structure. He showed that much of the weathered pyrochlore is very rich in K which he described and named kalipyrochlore (1978).

The general mineralogy of the deposit has been determined by colleagues at the Catholique University of Louvain, Belgium, and the chemistry by colleagues at the Ecole des Mines, St Etienne, France; work which will be published elsewhere and is described in an unpublished report (Albers *et al.*, 1994).

Petrography and mineralogy

Carbonatite

The calcite carbonatites are generally coarse-grained rocks of calcite, some ferroan dolomite, aegirine, phlogopite and microcline with accessory apatite, pyrochlore, magnetite, pyrrhotite and chalcopyrite.

Samples collected along the foot of the high cliffs on the northeastern side of Mutoro Hill contain up to 50% feldspar while some are rich in aegirine. The origin of these rocks is far from clear, but the abundant feldspar and aegirine is thought to derive from fenitized inclusions of country rocks. These rocks are particularly rich in fine-grained pyrochlore, more so than the normal carbonatite. Pyrochlore crystals up to several millimetres in diameter have been found and sampled from the upper parts of Mutoro Hill.

Laterite

The lower part of the weathering profile consists of moderately weathered material in which the major components are apatite, microcline and albite which are residual phases from the carbonatite, together with the secondary weathering products, goethite, crandallite and nacrite. Highly weathered material in the upper part of the profile consists mainly of goethite, crandallite, nacrite; although some areas are also quartz-rich. Pyrochlore is most abundant in the upper, more highly weathered ore.

Sample preparation and analytical procedures

Pyrochlore was analysed in samples of the lateritic ore from eight drill holes. Most samples were deslimed and then split into several size, magnetic, and density fractions; some unprocessed material was also examined. These samples, together with some large, octahedral single crystals collected from the laterite, were mounted in araldite blocks and polished in preparation for electron microprobe analysis. Fresh rocks were examined using polished thin sections.

Three electron microprobes at the Natural History Museum, London, were used during the course of this study. A Hitachi S2500 scanning electron microscope (SEM) equipped with a Link AN10/55S energy-dispersive (EDS) X-ray microanalysis system and operated at 15 kV accelerating voltage and 1 nA specimen current (vanadium calibration standard) was used to determine mineral textural relationships and for quantitative analysis of some pyrochlore. Two wavelength-dispersive (WDS) electron microprobes were used; initially, a Cambridge Instruments Microscan 9 operated at 20 kV and 25 nA probe current with a ZAF matrix correction, and subsequently a Cameca SX 50, operated at 20 kV and 20 or 25 nA with a PAP $\phi\rho z$ matrix correction programme. Standards used were a combination of well-characterized minerals, pure metals and synthetic compounds, including synthetic $NaNbO_3$. A sample of fresh Lueshe pyrochlore was analysed as a secondary standard to ensure consistency between techniques.
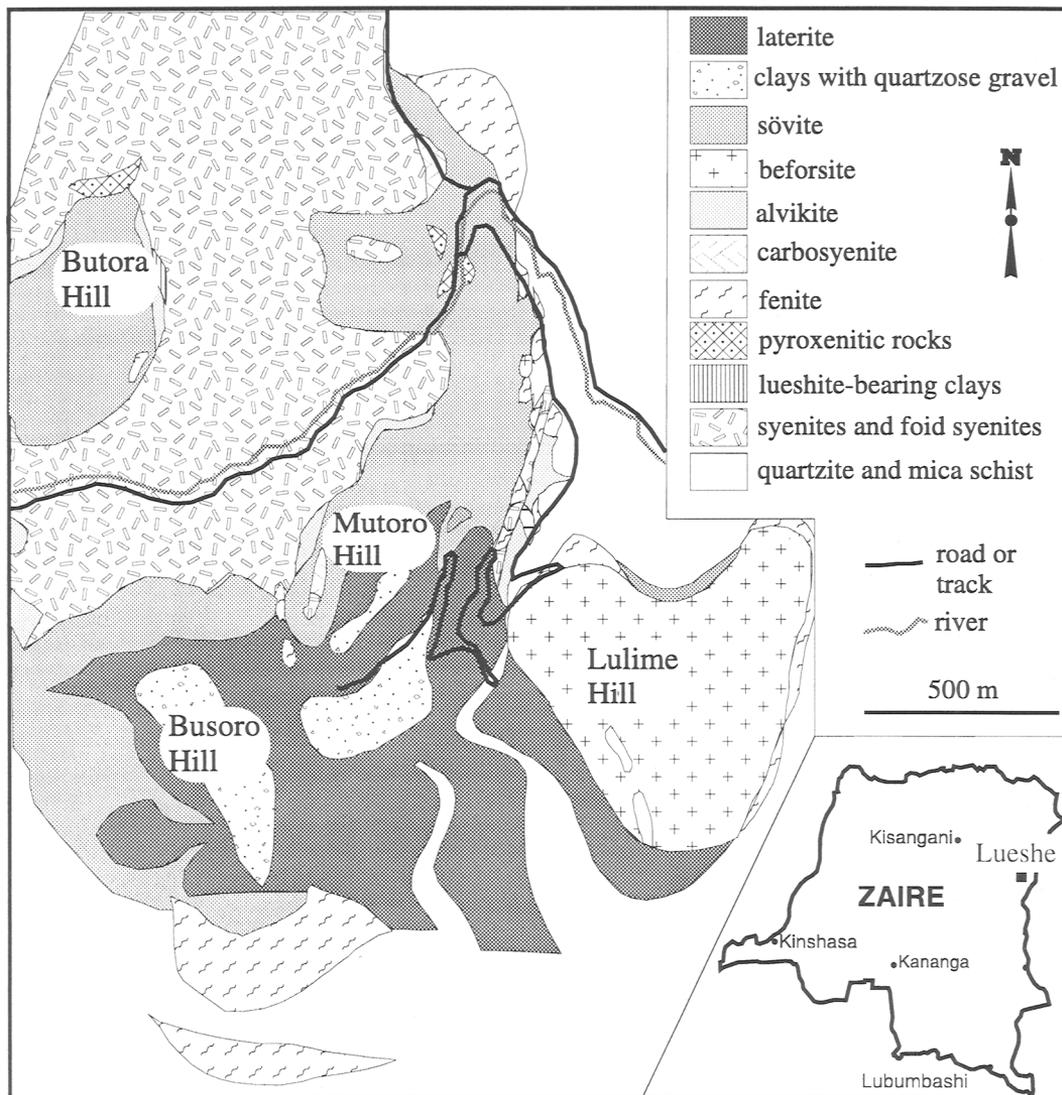
FIG. 1. Geological map of the Lueshe complex. Modified after Maravic *et al.* (1989).

Note on the calculation of pyrochlore formulae

The ideal formula for pyrochlore can be written as $(Ca,Na)_2Nb_2O_6(OH,F)$ with a more general formula $A_{2-x}B_2O_6(OH,F)_{1-y} \cdot zH_2O$ in which A can be Ca, Na, Sr, Ba, *REE*, U, Th, Mg, Mn and Sn and B includes Nb, Ti, Ta, and subordinate Si, Zr (Hogarth, 1989). In practice much weathered pyrochlore is strongly hydrated and has a large deficiency of A cations. Therefore, the formulae have been calculated to produce a total of 2 cations

in the B site. Cations have been variously assigned to A and B sites following the advice of D.D. Hogarth (pers. comm.) but there is some ambiguity concerning the correct assignment of Al, P and Fe. These elements are usually absent from fresh pyrochlore but are often present in the weathered varieties. Analyses with high concentrations of both Al and P (per cent levels) have been discounted as being contaminated by crandallite and high concentrations of Fe are thought to be caused by contamination from goethite. However, when the

concentrations are low, all of these elements have been assigned to the *B* site because of their atomic size and usual site occupancy, even though it is assumed that the *B* site is stable during weathering. If these elements were re-assigned to the *A* site or to secondary phases, the resulting increase in *A* cation totals would make only very small relative differences to the observed large deficiencies in the cation occupancy of this site. Water probably occupies the *A* site in weathered pyrochlore (Ercit *et al.* 1994, see discussion of kalipyrochlore below) but is not included in the term *A* cation as used here.

Pyrochlore in fresh carbonatite

Pyrochlore occurs as an accessory mineral in the carbonatite and is particularly abundant in the feldspar and aegirine-rich varieties. Its composition and textural relationships were determined in 16 fresh rocks in which it forms subhedral to euhedral crystals usually from <0.1 to 1 mm in diameter. Many crystals contain numerous inclusions of calcite, dolomite and/or apatite, as well as rutile and aegirine (Fig. 2a). Some crystals appear to have been partially remobilized and are now intergrown with dolomite and apatite (e.g. Fig. 2b).

Most pyrochlore in the fresh carbonatite has a composition close to the ideal formula $(Ca,Na)_2Nb_2O_6(F,OH)$ (Table 1) but there are some zoned and altered crystals which contain up to 1.88 wt.% SrO and 3 wt.% UO_2, particularly in the feldspar- and aegirine-rich carbonatites (Fig. 2b). Cation deficiencies in the *A* sites of the U- and Sr-bearing pyrochlore are observed to be as high as 50%. Oscillatory zoning in some crystals is thought to be of magmatic origin whereas more patchy alteration in others is thought to have occurred during a late magmatic or hydrothermal stage, or may be due to minor alteration following metamictization (Fig. 2b). The patchy zoning is considered not to be the first stage of weathering because the rock matrix is fresh. None of the fresh pyrochlore examined contains K or appreciable Ba.

Almost all of the Nb in the carbonatite occurs in the pyrochlore. Other very minor accessory Nb-rich minerals observed in the fresh carbonatite are ferrocolumbite $(Fe^{2+}Nb_2O_6)$, the rare mineral baotite, $Ba_4(Ti,Nb)_8Si_4O_{28}Cl$, and magnocolumbite, $(Mg,Fe^{2+},Mn)(Nb,Ta)_2O_6$. Analyses of these minerals are given in Table 2.

Pyrochlore in laterite derived from carbonatite

Pyrochlore occurs throughout the lateritic ore deposit but is particularly concentrated in crandallite-rich ore in the central and upper parts of the profile (Albers *et al.*, 1994).

Texture

Fracturing is ubiquitous in the pyrochlore (Fig. 2c and d) and most of the small grains appear to be fragments of larger crystals. In pyrochlore concentrates (notably non-magnetic fractions and density separates >3.31 g cm^{-3}) most grains are free of coatings of other minerals, but in other fractions there are many composite grains. The most widespread and abundant mineral associated with pyrochlore is crandallite, which occurs mantling many pyrochlore fragments and has formed within pyrochlore grains along fractures and in cavities (Fig. 2c and d). The admixture of pyrochlore and crandallite is seen in all ore types but its extent varies, being minor in apatitic and feldspathic ores and much more widespread in crandallitic ores. The composition of the crandallite is highly variable but usually intermediate between the crandallite and goyazite end members $(CaAl_3(PO_4)_2(OH)_5 \cdot H_2O - SrAl_3(PO_4)_2(OH)_5 \cdot H_2O)$ (Albers *et al.*, 1994). Pyrochlore also acts as a substrate for other minerals including goethite, clays and jarosite. Partial coatings of baryte were observed in a quartz-rich ore from the western part of the deposit.

Inclusions of probable pseudorutile and rutile are common in weathered pyrochlore but no remaining inclusions of carbonate minerals or apatite were observed. Relict concentric zoning, seen as crandallite replacement of original pyrochlore zones, is thought to represent the remains of Sr- and U-rich zones, as observed in the fresh pyrochlore (Fig. 2c and d).

Mineral chemistry

All analyses of weathered Lueshe pyrochlore have low totals suggesting extensive hydration, an observation in agreement with the analyses containing 10 wt.% H_2O presented by Van Wambeke (1965 and 1978). The *A* sites typically have site occupancies of between 0.15 and 0.59, when calculated to 2 *B* cations (Tables 3 and 4). The extent of the *A* site cation deficiency is emphasized on the ternary plot of Fig. 3.

Kalipyrochlore, low-Na pyrochlore, bariopyrochlore, strontiopyrochlore and ceriopyrochlore have all been observed at Lueshe (Tables 3 and 4). The most common compositional variations are conveniently represented in 2 dimensions on a ternary graph of K, Ba, and Ca+Na+Sr (Fig. 4). There is little variation in the *B* site cations; niobium being the predominant cation together with minor Ti.

Comparison with fresh pyrochlore

Weathered Lueshe pyrochlore has a much lower *A* site occupancy than the pyrochlore in fresh
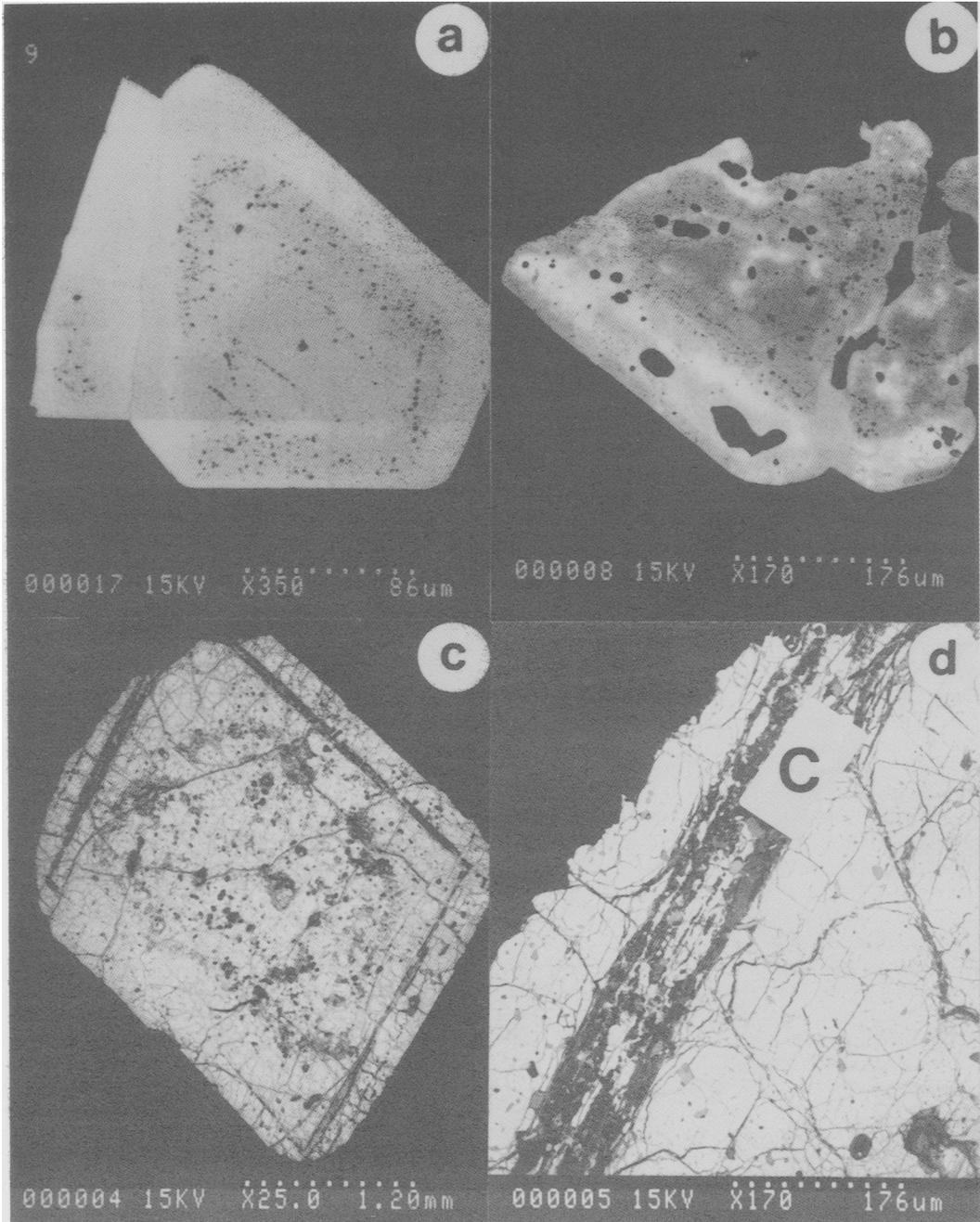
FIG. 2. Backscattered electron images (BSE) of pyrochlore from Lueshe. (*a*) Fresh, euhedral pyrochlore with inclusion-rich zones. (*b*) Fresh, zoned and partially remobilized pyrochlore. (*c*) BSE of a section through a weathered, octahedral pyrochlore crystal. There are many fractures, and inclusions of crandallite and Fe,Ti oxide. (*d*) BSE of an original zone in the pyrochlore crystal shown in (*c*) which has now been replaced by crandallite (C).

TABLE 1. Average compositions of pyrochlore from fresh carbonatite and fenite at Lueshe

Rock number Av. of.	Carbonatite BM 1991, P6						Fenite BM 1986, P22			
	(15) 32	(18) 18	(19) 17	(20) 16	(21) 14	(22) 4	(9) 17	(10) 19	(19) 20	(22) 23
Na_2O	7.06	8.01	7.52	7.51	8.21	6.64	5.06	5.22	7.86	7.82
Al_2O_3	0.05	0.06	0.08	0.10	0.05	<0.05	<0.05	<0.05	<0.05	<0.05
SiO_2	<0.05	<0.05	0.07	0.06	<0.05	0.16	0.16	0.21	<0.05	<0.05
CaO	17.87	14.95	15.52	15.82	15.08	11.52	14.23	12.79	15.89	16.23
TiO_2	3.01	2.29	3.54	3.63	3.79	3.82	4.57	4.42	3.84	3.83
MnO	<0.02	<0.02	0.02	0.02	<0.02	0.03	0.05	<0.02	<0.02	<0.02
Fe_2O_3	0.53	0.03	0.05	0.03	<0.03	0.21	0.36	0.24	0.17	0.22
SrO	0.60	1.44	1.54	1.39	1.47	1.39	1.21	1.35	1.12	0.96
ZrO_2	0.14	<0.05	<0.05	<0.05	<0.05	<0.05	<0.05	<0.05	<0.05	<0.05
Nb_2O_5	65.57	68.51	65.58	64.85	65.37	66.46	62.62	62.83	66.10	66.56
BaO	0.06	0.06	0.10	0.07	0.07	2.25	0.14	0.12	0.08	0.07
La_2O_3	<0.1	0.24	0.38	0.31	0.28	0.10	0.25	0.42	0.18	0.13
Ce_2O_3	<0.1	0.60	1.06	0.82	0.58	1.02	0.56	0.86	0.40	0.29
Ta_2O_5	2.03	0.26	0.37	0.44	0.56	0.17	1.13	0.96	0.05	0.03
PbO	0.28	<0.1	<0.1	<0.1	<0.1	<0.1	<0.1	<0.1	<0.1	<0.1
ThO_2	<0.1	0.10	0.54	0.48	<0.1	0.10	0.39	0.27	0.12	<0.1
UO_2	0.09	0.04	0.05	0.11	0.08	1.22	2.47	3.11	0.14	0.08
F	4.73	4.67	4.38	4.40	4.75	3.67	3.52	3.42	4.56	5.00
total	102.02	101.28	100.84	100.05	100.32	98.78	96.74	96.25	100.56	101.25
O=F	1.99	1.96	1.84	1.85	2.00	1.54	1.48	1.44	1.92	2.11
Total	100.02	99.32	98.99	98.20	98.32	97.23	95.26	94.81	98.64	99.15

Formula calculated to 2 B site cations
A site

Na	0.830	0.945	0.894	0.900	0.976	0.774	0.604	0.625	0.926	0.915
Ca	1.161	0.975	1.020	1.047	0.991	0.742	0.939	0.847	1.035	1.049
Mn			0.001	0.001		0.002	0.003			
Sr	0.021	0.051	0.055	0.050	0.052	0.048	0.043	0.048	0.040	0.034
Ba	0.001	0.001	0.002	0.002	0.002	0.053	0.003	0.003	0.002	0.002
La	0.000	0.005	0.009	0.007	0.006	0.002	0.006	0.010	0.004	0.003
Ce	0.000	0.013	0.024	0.019	0.013	0.022	0.013	0.019	0.009	0.006
Pb	0.005									
Th		0.001	0.008	0.007		0.001	0.006	0.004	0.002	
U	0.001	0.001	0.001	0.002	0.001	0.016	0.034	0.043	0.002	0.001
Total	2.019	1.993	2.013	2.034	2.042	1.661	1.650	1.599	2.019	2.010

B site

Al	0.004	0.004	0.006	0.007	0.004					
Si			0.004	0.004		0.010	0.010	0.013		
Ti	0.137	0.105	0.163	0.169	0.175	0.173	0.212	0.205	0.176	0.174
Fe	0.024	0.001	0.002	0.001	0.000	0.010	0.017	0.011	0.008	0.010
Zr	0.004									
Nb	1.797	1.885	1.818	1.812	1.812	1.806	1.743	1.754	1.816	1.816
Ta	0.034	0.004	0.006	0.010	0.009	0.003	0.019	0.016	0.001	0.001
Total	2.000	2.000	2.000	2.000	2.000	2.000	2.000	2.000	2.000	2.000
Total O	6.507	6.474	6.498	6.510	6.473	6.203	6.269	6.227	6.470	6.461
F	0.907	0.899	0.850	0.860	0.921	0.698	0.686	0.668	0.876	0.954

Analyses by electron microprobe (see text for details).
Total Fe as Fe_2O_3
Total Ce as Ce_2O_3

TABLE 2. Electron microprobe analyses of baotite, $Ba_4(Ti,Nb)_8Si_{14}O_{28}Cl$, ferrocolumbite, $Fe^{2+}Nb_2O_6$, and magnocolumbite, $(Mg,Fe^{2+},Mn)(Nb,Ta)_2O_6$, from Lueshe carbonatite

| | Baotite | | Ferrocolumbite | Magnocolumbite |
	low-Nb	high-Nb	1 analysis	Mean of 5
Na_2O	0.08	0.04	<.05	<.05
MgO	<.05	<.05	0.50	6.30
Al_2O_3	0.42	0.40	<.05	<.05
SiO_2	14.00	13.35	<.05	<.05
CaO	0.01	0.03	0.15	0.09
TiO_2	20.16	7.89	2.12	1.65
MnO	—	—	0.64	0.46
Fe_2O_3	5.23	8.83	19.50*	9.60*
SrO	0.27	0.11	<0.1	<0.1
Nb_2O_5	18.83	30.18	75.97	81.16
BaO	37.74	35.75	<0.1	0.11
Ta_2O_5	0.47	0.47	<0.2	<0.2
F	<.05	—	—	—
Cl	2.18	2.07	—	—
Total	99.39	99.12	98.88	99.37
O=Cl	0.50	0.47	—	—
Total	98.91	98.65	98.88	99.37

Formulae

	calculated to 28(O)			calculated to 6(O)	
Si	3.858	3.822	Mg	0.042	0.502
Al	0.136	0.135	Ca	0.009	0.005
Total	3.994	3.957	Mn	0.030	0.021
			Fe^{2+}	0.916	0.429
Ti	4.178	1.698	Ba		0.002
Nb	2.346	3.906	Total	0.997	0.959
Ta	0.035	0.037			
Fe^{3+}	1.085	1.902	Ti	0.090	0.066
Total	7.644	7.543	Nb	1.929	1.962
			Total	2.019	2.028
Ba	4.076	4.010			
Ca	0.003	0.009	O	6.000	6.000
Sr	0.043	0.018			
Total	4.122	4.037			
Cl	1.018	1.004			
O	28.000	28.000			

* total Fe as FeO
— not analysed

carbonatite, as illustrated by Fig. 3. The main changes during weathering are the leaching of Ca and Na from the A site and their partial replacement by Ba, K, Sr and, probably, water (which was not measured and therefore is not included in the A totals). Although the U- and Sr-bearing pyrochlore in fresh rock is also A cation-deficient (Fig. 3), it is thought not to represent the weathering path because it occurs in primary, oscillatory zones. Therefore, no intermediate compositions have been observed and

the transition zone must occur at the interface with fresh rock, which is probably not represented in the drill hole material.

Kalipyrochlore

Lueshe is unique in that the most abundant pyrochlore is kalipyrochlore. Such K-rich pyrochlore was first reported by Van Wambeke (1978, 1965) from Lueshe and has not been reported from any

TABLE 3. Selected electron microprobe analyses of kalipyrochlore from laterite overlying carbonatite at Lueshe, arranged in order of increasing A cation depletion.

Number	Kalipyrochlore							Kalipyrochlore with extreme A site depletion			
	1 C11,17	2 C11,18	3 E25.DR298	4 E43.PY83	5 E206,75	6 E204,59	7 E200,26	8 E158 D	9 E185,14	10 E198,4	11 E198,2
Na_2O	0.50	0.22	–	–	0.03	0.02	0.02	0.03	–	–	–
MgO	–	–	–	0.24	–	–	–	–	0.09	–	–
Al_2O_3	0.43	–	–	–	–	0.05	0.03	0.97	0.03	0.09	0.11
SiO_2	0.01	–	–	–	0.01	0.01	–	0.65	0.21	0.02	0.09
P_2O_5	0.58	–	–	–	–	0.03	–	0.23	–	0.05	–
K_2O	6.47	3.67	2.23	4.03	2.69	2.92	1.46	0.19	0.55	0.98	0.20
CaO	1.03	0.80	0.62	0.36	0.26	0.17	0.42	1.28	1.16	0.21	0.26
TiO_2	3.43	2.94	3.25	2.81	4.03	3.37	1.90	2.87	3.42	3.99	5.32
MnO	–	–	–	–	–	–	–	0.02	–	–	–
Fe_2O_3	–	0.06	0.40	1.09	0.14	1.28	1.29	1.91	1.42	1.86	2.20
SrO	0.03	2.59	1.18	–	3.86	0.18	0.13	1.72	0.16	–	0.09
ZrO_2	–	–	–	–	0.02	–	0.15	0.00	0.05	–	0.20
Nb_2O_5	72.98	76.64	73.97	80.15	76.41	79.82	80.80	83.46	81.74	82.08	86.78
BaO	0.63	0.63	7.22	1.05	0.11	0.14	1.27	0.21	0.58	0.16	0.49
La_2O_3	0.02	0.05	–	–	0.06	0.10	–	0.04	–	0.09	0.30
Ce_2O_3/CeO_2	0.13	0.07	–	–	–	–	0.17	0.03	0.14	0.09	0.12
Ta_2O_5	–	–	–	–	–	0.08	2.31	–	0.01	0.12	–
ThO_2	–	0.07	–	–	–	–	–	–	–	–	–
UO_2	1.05	0.54	–	–	0.15	–	0.12	0.34	0.06	–	0.01
F	0.20	0.03	–	–	0.03	–	0.08	–	0.03	0.13	0.03
Total	87.49	88.31	88.87	89.73	87.80	88.17	90.15	93.95	89.65	89.87	96.20

TABLE 3. (cont.)

	1	2	3	4	5	6	7	8	9	10	11
	C11,17	C11,18	E25,DR298	E43,PY83	E206,75	E204,59	E200,26	E158 D	E185,14	E198,4	E198,2
Formula calculated to 2 B site cations											
A site											
Na	0.053	0.023			0.003	0.002	0.002	0.003			
Mg				0.018					0.007		
K	0.451	0.254	0.157	0.263	0.182	0.188	0.094	0.011	0.034	0.060	0.011
Ca	0.060	0.047	0.037	0.020	0.015	0.009	0.023	0.063	0.061	0.011	0.012
Mn								0.001			
Sr	0.001	0.081	0.038	0.000	0.119	0.005	0.004	0.046	0.005		0.002
Ba	0.014	0.013	0.156	0.021	0.002	0.003	0.025	0.004	0.011	0.003	0.009
La	0.000	0.001			0.001	0.002		0.001		0.002	0.005
Ce	0.003	0.001					0.003	0.001	0.002	0.002	0.002
Th		0.001									
U	0.013	0.007			0.002		0.001	0.004	0.001		
Total	0.593	0.399	0.375	0.321	0.282	0.207	0.150	0.116	0.112	0.078	0.036
Al	0.028					0.001		0.053		0.005	0.006
Si	0.001				0.001	0.001		0.030		0.001	0.004
P	0.027							0.009	0.010	0.002	
Ti	0.141	0.120	0.135	0.108	0.161	0.128	0.072	0.100	0.126	0.144	0.177
Fe		0.002	0.017	0.042	0.006	0.049	0.049	0.066	0.052	0.067	0.073
Zr					0.001		0.004		0.001		0.004
Nb	1.803	1.878	1.848	1.850	1.833	1.818	1.842	1.742	1.806	1.779	1.739
Ta						0.001	0.032			0.002	
Total	2.000	2.000	2.000	2.000	2.000	2.000	2.000	2.000	2.000	2.000	2.000
total O	5.258	5.236	5.225	5.094	5.147	4.999	5.018	4.946	4.983	4.904	4.868
F	0.035	0.005			0.005		0.013		0.005	0.020	0.004

Total Fe as Fe_2O_3. Total Ce as Ce_2O_3. – not detected.

TABLE 4. Selected electron microprobe analyses of low-Na pyrochlore and bario-, strontio- and ceriopyrochlore from laterite overlying carbonatite at Lueshe

Number	Low-Na pyrochlore			Bariopyrochlore					Strontiopyrochlore			Ceriopyrochlore	
	1 G8 GA7	2 E173,149	3 E196,2	4 E194,20	5 E194,16	6 E54FW141	7 E17,DR153	8 E20,DR219	9 E166,4	10 E208,96	11 E173,164	12 E208,86	13 E161,68
Na_2O	0.04	0.06	0.01	0.15	0.08	0.31	–	–	0.67	0.12	0.16	0.34	0.89
MgO	–	–	–	–	0.04	–	–	–	–	–	–	–	–
Al_2O_3	–	0.02	0.19	0.17	0.03	–	0.57	–	0.03	0.02	0.01	0.07	0.52
SiO_2	0.17	0.01	0.44	–	–	–	–	–	–	–	–	0.01	0.10
P_2O_5	0.03	0.03	–	–	–	–	–	–	0.06	–	–	–	–
K_2O	0.30	1.15	0.50	1.19	1.25	0.22	1.78	0.22	0.52	1.76	1.91	1.72	0.73
CaO	7.44	3.30	0.91	1.36	2.12	0.21	0.89	–	0.27	1.70	0.47	2.70	4.19
TiO_2	2.61	4.53	4.77	3.73	4.64	1.69	2.68	2.56	3.79	4.03	3.86	2.96	2.31
MnO	–	–	–	–	–	–	–	–	0.03	–	–	–	0.03
Fe_2O_3	0.28	0.04	1.25	1.28	0.62	–	4.23	1.31	–	0.71	–	0.55	–
SrO	0.08	2.03	0.74	0.86	0.94	3.27	–	1.75	5.76	6.60	7.21	3.82	0.32
ZrO_2	–	0.03	0.05	0.09	–	–	–	–	–	0.08	0.02	0.02	–
Nb_2O_5	80.49	77.18	75.19	72.05	74.13	70.77	72.86	70.87	72.32	76.10	74.07	69.77	60.54
BaO	0.80	0.12	1.47	10.09	6.57	14.57	7.31	14.93	4.95	0.24	1.13	0.90	0.12
La_2O_3	0.04	0.04	0.02	0.03	0.08	–	–	–	–	–	–	0.02	–
Ce_2O_3/CeO_2	0.05	1.96	0.04	0.47	0.19	–	–	–	0.30	0.89	0.24	11.00	15.44
Ta_2O_5	–	0.19	–	0.03	0.21	–	–	–	0.08	0.15	0.11	–	–
PbO	–	2.63	–	–	–	–	–	–	0.46	–	0.34	–	1.67
ThO_2	–	0.05	–	0.02	0.11	–	–	–	0.20	–	0.09	–	0.10
UO_2	–	0.18	0.84	–	0.03	–	–	–	–	0.05	0.17	0.06	0.21
F	–	0.06	0.18	–	–	–	–	–	–	–	0.11	–	0.10
Total	92.33	93.61	86.60	91.52	91.04	91.04	90.32	91.64	89.44	92.45	89.90	93.94	87.27

TABLE 4. (cont.)

	1 G8 GA7	2 E173,149	3 E196,2	4 E194, 20	5 E194,16	6 E54FW141	7 E17,DR153	8 E20,DR219	9 E166,4	10 E208,96	11 E173,164	12 E208,86	13 E161,68
Formula calculated to 2 B site cations													
A site													
Na	0.004	0.006	0.001	0.016	0.008	0.036			0.073	0.012	0.017	0.039	0.116
Mg					0.003								
K	0.020	0.076	0.033	0.083	0.085	0.017	0.117	0.016	0.037	0.118	0.134	0.128	0.062
Ca	0.411	0.184	0.050	0.080	0.121	0.014	0.049		0.016	0.096	0.028	0.169	0.301
Mn									0.001				0.002
Sr	0.002	0.061	0.022	0.027	0.029	0.114		0.044	0.187	0.201	0.230	0.129	0.012
Ba	0.016	0.002	0.029	0.216	0.137	0.343	0.148	0.336	0.109	0.005	0.024	0.021	0.003
La	0.001	0.001		0.001	0.002								
Ce	0.001	0.037	0.001	0.009	0.004				0.006	0.017	0.005	0.224	0.362
Pb		0.037							0.007		0.005		0.030
Th		0.001							0.003		0.001		0.002
U		0.002	0.010		0.001					0.001	0.002	0.001	0.003
Total	0.455	0.408	0.145	0.432	0.390	0.524	0.314	0.396	0.440	0.450	0.445	0.710	0.893
B site													
Al	0.009	0.001	0.011	0.011	0.002		0.035		0.002	0.001	0.001	0.005	0.041
Si	0.001	0.001	0.022									0.001	0.007
P	0.001	0.001							0.003				
Ti	0.101	0.177	0.183	0.153	0.186	0.076	0.104	0.111	0.160	0.159	0.159	0.130	0.117
Fe	0.011	0.002	0.048	0.053	0.025		0.164			0.028	0.001	0.024	
Zr		0.001	0.001	0.002				0.049		0.002		0.001	
Nb	1.878	1.815	1.734	1.780	1.784	1.924	1.698	1.840	1.834	1.807	1.838	1.840	1.836
Ta		0.003			0.003				0.001	0.002	0.002		
Total	2.000	2.000	2.000	2.000	2.000	2.000	2.000	2.000	2.000	2.000	2.000	2.000	2.000
Total O	5.379	5.296	4.976	5.247	5.228	5.459	5.005	5.308	5.308	5.284	5.295	5.758	6.067
F	0.010	0.010	0.029	0.005	0.005						0.019		0.021

Ce as Ce^{4+} and CeO_2 in analyses 12,13, as Ce^{3+} and Ce_2O_3 in the other analyses. − not detected. Total Fe as Fe_2O_3
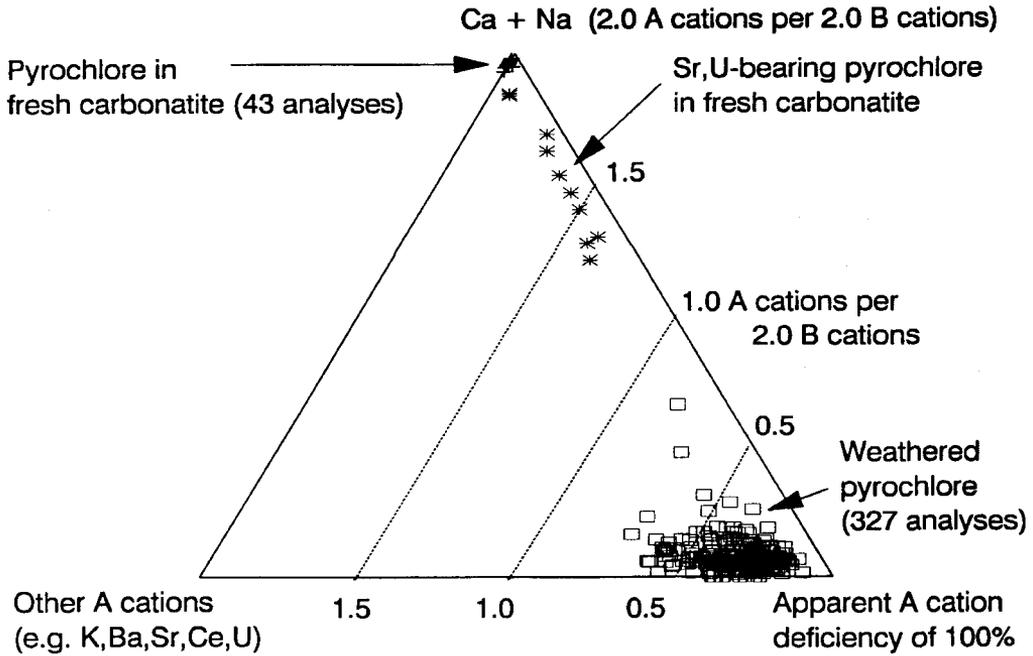
FIG. 3. A cation occupancy of Lueshe pyrochlore. The cations have been calculated to 2 B site cations according to a formula of $A_{2-x}B_2O_6(OH,F)_{1-y}\cdot zH_2O$. (see Tables 1 and 2).

other locality (see also Fig. 9). It is always strongly hydrated and A cation-deficient. A recent structure refinement by Ercit *et al.* (1994) resulted in a suggested structural formula of $([H_2O]_{0.99}Sr_{0.05}Ca_{0.01})_{\Sigma 1.05}(Nb_{1.80}Ti_{0.20})_{\Sigma 2}(O_{4.06}OH_{1.94})_{\Sigma 6}([H_2O]_{0.86}K_{0.14})$ and an empirical formula of $Nb_2(O,OH)_6\cdot pH_2O$ where p is <1.75. Calculated on an anhydrous basis to 2 B cations, the analyses presented in Table 3 have between 5.26 and 4.87 oxygen atoms, depending on the degree of A cation depletion. A total of 5 oxygen atoms would be equivalent in charge to $(O)_4(OH)_2$, which is in reasonable agreement with the suggested formula of Ercit *et al.*(1994). The least A cation-depleted analyses in Table 3 have the highest (O) values and are therefore believed to represent the transition from fresh pyrochlore. The most leached compositions have close to 5 oxygens; the exception being one analysis (Table 3, anal. 11) which, having an exceptionally low total of A cations and a much higher analysis total than is usual for kalipyrochlore, may be a different mineral species. If this is kalipyrochlore, it would represent the lowest observed A site occupancy (0.036). Apart from this composition, the lowest observed A site occupancy is 0.078 (Table 3, anal. 10). There are always some

residual A cations, even in the most leached compositions so that although there are compositions very close to the empirical formula suggested by Ercit *et al.*(1994), there are none which are an exact match.

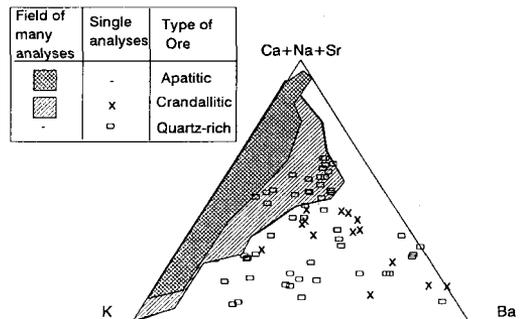Analyses of the <5 μm fraction from the standard desliming process indicate that the smallest grains are

FIG. 4. Chemical variation in weathered Lueshe pyrochlore. Regardless of the ratio of K:(Ca+Na+Sr), Ba tends to increase from apatitic (least weathered) to crandallitic to quartz-rich (most weathered) lateritic ore.

more *A* cation-depleted (Table 3, anals 8 and 9) than the larger fragments.

The Ba, Sr and Ca contents of kalipyrochlore are variable and not directly related to the K content or the degree of *A* site depletion (Fig. 4 and Table 3).

Bariopyrochlore

Bariopyrochlore is a far more common component of weathered carbonatites than kalipyrochlore. It is the most abundant pyrochlore in the world's largest deposit at Araxá, Brazil (Issa Filho *et al.*, 1984), was first described from weathered biotite rock at a carbonatite contact at Panda Hill, Tanzania (Jäger *et al.*, 1959), and is also reported from weathered carbonatite at Bingo, Zaire (Van Wambeke, 1971). However, at Lueshe it is very much subsidiary to the kalipyrochlore and localized (see below). The maximum recorded Ba in Lueshe pyrochlore is 14.93 wt.% BaO (Table 4, anal. 8) but compositions with > 6.5 wt.% BaO also classify as bariopyrochlore. Potassium, strontium and calcium levels are variable (Table 4, Fig. 4).

Strontium-bearing pyrochlore and strontiopyrochlore

A small but variable amount of Sr is present in much of the pyrochlore at Lueshe, including the kalipyrochlore (Tables 3 and 4). Occasionally, analyses have formulae which classify, according to the nomenclature of Hogarth (1989), as the Sr end member, now usually called strontiopyrochlore (Table 4, anals 9–11) although the mineral name has not been approved officially by the International Mineralogical Association (Jambor *et al.* 1988; Clark, 1993; Nickel and Nichols, 1991; Fleischer and Mandarino, 1991).

Strontiopyrochlore is also common in other weathered carbonatites, for example at Mt Weld (Lottermoser and England, 1988), Enisei Ridge, Russia (Lapin *et al.*, 1988) and in other Siberian carbonatites described by Lapin and Kulikova (1989).

Low-Na pyrochlore

An unusual, intermediate composition of calcium-rich, sodium-depleted pyrochlore was found in jarosite-rich crandallitic ore (Table 4, anal. 1). The sodium has been completely removed but nearly half the Ca (7 wt.% CaO, 0.414 Ca per 2 B cations) remains and there has been little uptake of other cations. No zoning was detected in these grains. In this area of the orebody, potassium occurs in the secondary sulphate jarosite ($KFe_3(SO_4)_2(OH)_6$) rather than kalipyrochlore.

Other similar pyrochlore is more highly *A* cation-depleted, contains higher levels of K and Sr (Table 4, anals 2 and 3) and is a variant on the kalipyrochlore associated with it.

Ceriopyrochlore

Narrow mantles of ceriopyrochlore were observed on some pyrochlore grains from apatitic ore near the base of several drill holes and also on some large, octahedral pyrochlore crystals (Fig. 5). Although CeO_2 contents of up to 20 wt.% have been found (Table 5), the other *REE* oxides are below 0.2 wt.% suggesting fractionation of Ce from the other *REE* during weathering, probably as a result of oxidation to Ce^{4+}. Apart from the Ce, there is little variation between the core and mantle of individual crystals, although there may be significant differences in the composition of separate crystals from any particular locality (e.g. SrO, Table 5). At about 0.7 (Table 5), the *A* cation totals of the ceriopyrochlore rims are much higher than the kalipyrochlore cores (Table 5). It is thought that the ceriopyrochlore represents a re-absorption of cations back into the pyrochlore structure.

Ceriopyrochlore is not the major host for *REE* in the weathered carbonatite. Low levels of *REE* in abundant crandallite-goyazite and grains of rhabdophane found as inclusions in goethite and crandallite probably fulfil this role.

Zoning and variation

Apart from the mantles of ceriopyrochlore, very little zoning within individual pyrochlore grains has been observed, even within 5 mm diameter, octahedral crystals. However, it is common to find individual crystals of kali- to strontio- or bariopyrochlore within a metre of each other.

Final breakdown products

Although Nb was detected in some goethite analyses, it was often difficult to discriminate between Nb incorporated into the goethite structure and inclusions of pyrochlore, which were as small as 1 mm, enclosed in goethite. However, in some samples taken from 0–18 m depth, i.e. in the most highly weathered part of one of the profiles, the presence of Nb in goethite occurring as anhedral inclusions in crandallite was unambiguous. Levels of Nb_2O_5 varied up to 13 wt.% (Table 6). Between 1.4 and 3 wt.% Nb_2O_5 was also found in goethite from highly weathered ores towards the top of Mutoro Hill.

Accessory amounts of ferrocolumbite were found as inclusions in crandallite and goethite and as
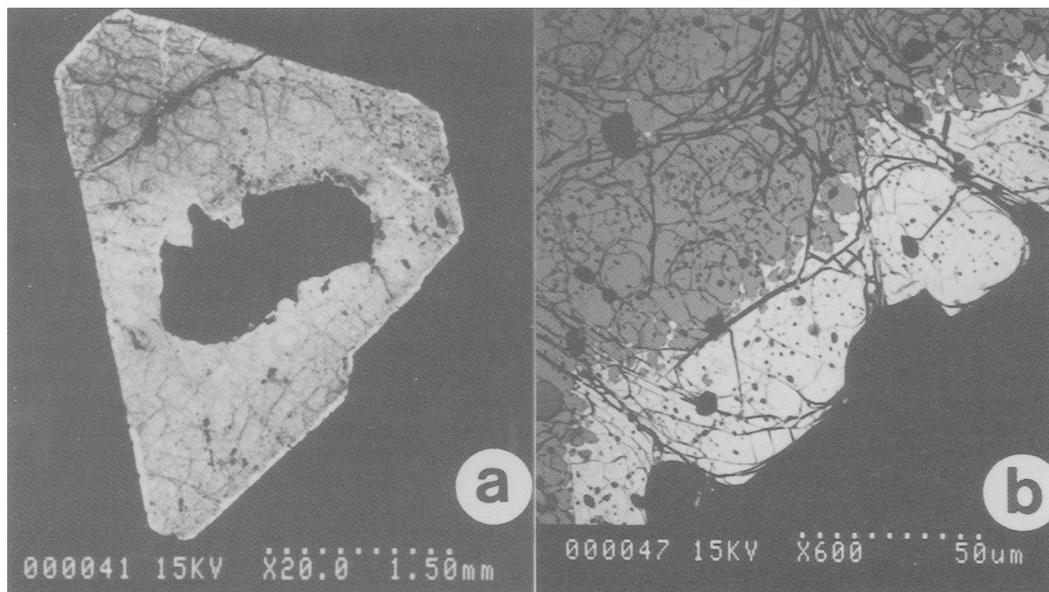
FIG. 5. (*a*) Backscattered electron images of kalipyrochlore showing a narrow mantle of ceriopyrochlore (white). (*b*) Higher magnification image of the ceriopyrochlore mantle. The *A* cation total in the kalipyrochlore is 0.2 per 2 *B* site cations. The *A* cation total in the ceriopyrochlore is 0.7 atoms per formula unit.

occasional pyrochlore alteration products. In addition, Van Wambeke (1965) reported pseudomorphs of ferrocolumbite after pyrochlore. However, not all columbite is a pyrochlore weathering product, some was identified in fresh carbonatite (see above).

Generally, therefore, pyrochlore is stable throughout the weathering profile despite the large amount of *A* cation leaching. However, when it does finally break down, the mineral hosts for the Nb are goethite and possibly ferrocolumbite. Presumably some Nb is also removed in groundwater but no analyses of local waters were made during the course of this study. In contrast to Lottermoser and England (1988), we have found no evidence that Nb enters the crandallite structure.

Chemical variation of pyrochlore through the deposit

The pyrochlore composition varies laterally across the deposit and with depth within the weathering profile. An example of changes within a typical profile is shown in terms of average *A* cations and average Nb_2O_5 wt.% in Fig. 6*a* and *b*. The wt.% Nb_2O_5 is an important economic factor, and varies in relation to the *A* cations. High atomic number *A* cations, e.g. Ba, produce low wt.% Nb_2O_5 whereas 'lighter' *A* cations, e.g. K, produce higher wt.% Nb_2O_5. Although the profiles are not identical in each drill hole, there is a general tendency for the least weathered (i.e. deepest) part of the profile, which contains mainly residual primary phases such as apatite and feldspar, to contain the least *A* cation-depleted pyrochlore and lowest Nb_2O_5 values (Fig. 6). This pattern is modified by variations in Sr and Ba which greatly influence the Nb_2O_5 wt.%. The most *A* cation-depleted, highest-Nb pyrochlore normally occurs near the centre of the profile (Fig. 6*a* and *b*) but near the surface the *A* site occupancies tend to rise again and Ba contents increase (Fig. 6*a*). The most K-rich, highest-Nb pyrochlore occurs at intermediate levels in the drill holes but throughout a drill hole in the centre of the deposit. The most Ba-rich pyrochlore occurs in quartz- and clay-rich ores and also close to the surface in some other drill holes (Fig. 7*a*). In contrast, the highest levels of Sr occur in the Ba-rich pyrochlore and also near the base of the profiles throughout the deposit (Fig. 7*b*).

Discussion of the causes of chemical variation in the Lueshe weathered pyrochlore

No single process can account for all the variation in pyrochlore composition observed in the Lueshe orebody. A number of different processes, thought to operate to a greater or lesser degree are discussed below.

TABLE 5. Selected electron microprobe analyses of two euhedral, weathered. Lueshe kalipyrochlore crystals which have outer zones of ceriopyrochlore

	Grain B				Grain E			
	Sr-bearing kalipyrochlore		Ceriopyrochlore		Kalipyrochlore		Ceriopyrochlore	
Na_2O	0.03	0.10	0.48	0.36	0.05	0.02	0.09	0.15
MgO	0.01	–	–	0.02	0.01	–	--	–
Al_2O_3	0.03	0.04	–	0.01	–	0.02	–	–
K_2O	2.94	1.78	2.29	2.17	3.99	2.72	2.08	3.04
CaO	0.03	0.02	0.03	0.04	0.01	–	0.04	0.01
TiO_2	3.76	3.96	3.70	3.65	2.16	4.24	3.14	2.85
MnO	0.04	0.01	–	–	–	–	–	–
Fe_2O_3	0.11	0.44	–	–	0.03	–	–	–
SrO	2.82	2.49	2.98	2.93	0.25	0.43	0.47	0.65
ZrO_2	0.15	0.22	0.18	0.12	–	0.05	0.09	–
Nb_2O_5	75.45	75.16	62.67	64.66	77.53	75.75	63.97	62.32
BaO	0.20	0.10	–	–	0.22	0.10	–	–
La_2O_3	0.04	–	0.08	0.12	–	0.02	0.09	0.05
CeO_2	0.13	0.18	18.69	19.35	0.13	0.12	19.63	18.37
Pr_2O_3	–	0.02	–	–	0.18	0.13	–	0.02
Nd_2O_3	0.05	0.05	0.15	–	–	0.05	0.05	–
Ta_2O_5	0.05	0.14	–	–	0.04	–	0.01	–
PbO	–	–	0.52	0.39	–	–	0.10	0.17
ThO_2	–	0.13	–	0.02	–	–	–	–
UO_2	0.04	0.12	–	0.01	0.06	0.02	–	–
Total	85.89	84.96	91.77	93.85	84.66	83.67	89.76	87.63

Formula calculated to 2 B site cations

A site								
Na	0.003	0.010	0.060	0.044	0.005	0.002	0.011	0.019
Mg	0.001			0.002	0.001			
K	0.202	0.121	0.187	0.173	0.277	0.185	0.169	0.256
Ca	0.002	0.001	0.002	0.003	0.001		0.003	0.001
Mn	0.002	0.001						
Sr	0.088	0.077	0.111	0.106	0.008	0.013	0.017	0.025
Ba	0.004	0.002			0.005	0.002		
La	0.001		0.002	0.003		0.000	0.002	0.001
Ce^{4+}	0.003	0.004	0.418	0.422	0.003	0.002	0.438	0.423
Pr		0.000			0.004	0.003		0.001
Nd	0.001	0.001	0.003			0.001	0.001	
Pb			0.009	0.007			0.002	0.003
Th		0.002		0.000				
U	0.001	0.001		0.000	0.001			
Total	0.307	0.220	0.792	0.758	0.303	0.209	0.643	0.729

B site								
Al	0.002	0.003		0.001		0.001		
Ti	0.152	0.159	0.178	0.171	0.089	0.170	0.151	0.141
Fe	0.005	0.018			0.001			
Zr	0.004	0.006	0.006	0.004		0.001	0.003	
Nb	1.837	1.813	1.816	1.824	1.910	1.827	1.846	1.859
Ta	0.001	0.002			0.001		0.000	
Total	2.000	2.000	2.000	2.000	2.000	2.000	2.000	2.000
Total O	5.123	5.059	5.998	5.985	5.122	5.033	5.915	5.944

Total Fe as Fe_2O_3: Total Ce as CeO_2; – not detected

TABLE 6. Selected electron microprobe analyses of Nb-bearing goethite from laterite overlying carbonatite at Lueshe

| | | C85,E166b | | | B33, E18 |
	FW204	FW207	FW210	FW217	DR274
Na$_2$O	0.58	–	0.45	–	0.35
MgO	–	–	–	–	1.59
Al$_2$O$_3$	2.69	3.55	3.82	8.81	1.21
SiO$_2$	1.71	2.01	2.21	2.79	2.63
P$_2$O$_5$	2.32	1.60	1.51	7.53	–
K$_2$O	–	–	–	0.17	–
CaO	0.26	0.23	0.27	1.47	0.25
TiO$_2$	2.12	1.23	1.26	2.97	0.33
MnO	–	–	–	–	1.51
Fe$_2$O$_3$	70.68	72.77	69.30	43.36	80.82
SrO	–	–	–	2.24	–
Nb$_2$O$_5$	7.24	4.03	1.97	13.74	1.33
Total	87.60	85.42	80.79	83.08	90.02

All analyses were obtained using an energy-dispersive spectrometer.
Total Fe as Fe$_2$O$_3$
– not detected

Leaching of A cations and the progressive fracturing of pyrochlore crystals are responsible for the major change from fresh Ca, Na pyrochlore to weathered kali- and strontiopyrochlore, the trend of decreasing A cations and increasing Nb$_2$O$_5$ near the base of the weathering profile, the extreme A cation depletion seen in some grains (especially <20 μm grains) and the final breakdown of pyrochlore to Nb-bearing goethite.

Fresh pyrochlore composition determines the Nb and Ti contents of the weathered pyrochlore at Lueshe (compare fresh and weathered compositions in Tables 1,3,4 and 5) but has little influence on the A cations, apart possibly from small variations in Sr observed in fresh pyrochlore and the fact that U-bearing fresh pyrochlore appears more susceptible to weathering than pyrochlore *s.s.* (Fig. 2*d*).

Initial carbonatite mineralogy and bulk chemistry probably has an important influence on the composition of the weathered pyrochlore. The main source of potassium is K-feldspar (microcline) which is locally abundant in parts of the carbonatite. It is also present together with kalipyrochlore in the deepest parts of the weathering profile, suggesting that potassium is mobile in the laterite and has been derived from feldspar breakdown at higher levels. The high proportion of K-feldspar included in the carbonatite is a particular characteristic of Lueshe.

Potassium feldspar could also be an important source of Ba. The differing distribution of K and Ba-rich pyrochlore may be explained if the more mobile

potassium cation has moved downwards through the weathering profile to enter pyrochlore at deeper levels, whereas the less mobile Ba has remained closer to its source.

Cation exchange and uptake could be another factor in the production of Ba-rich pyrochlore towards the top of some of the weathering profiles at Lueshe. It is noticeable that Ba contents (and also A cation totals) tend to be higher towards the top of the profiles. This enrichment may be coincidental with the variations described above or may be due, at least in part, to cation exchange and uptake by the pyrochlore, such that kalipyrochlore from the centre of the profile is converted to bariopyrochlore. The high speed with which pyrochlore may undergo cation exchange under ambient conditions was demonstrated during the present work by the absorption of thallium by kalipyrochlore during a density separation with thallium-bearing heavy liquid, unintentionally repeating experiments by van der Veen (1963).

Erosion of weathered material from the deeply incised east part of the Lueshe orebody may have eroded the upper, more highly weathered parts containing bariopyrochlore (Fig. 7*a*).

Weathering trends in other carbonatites

Leaching of the A cations appears to be common to all pyrochlore weathering, similar changes having been reported at Mt Weld (Lottermoser and England,
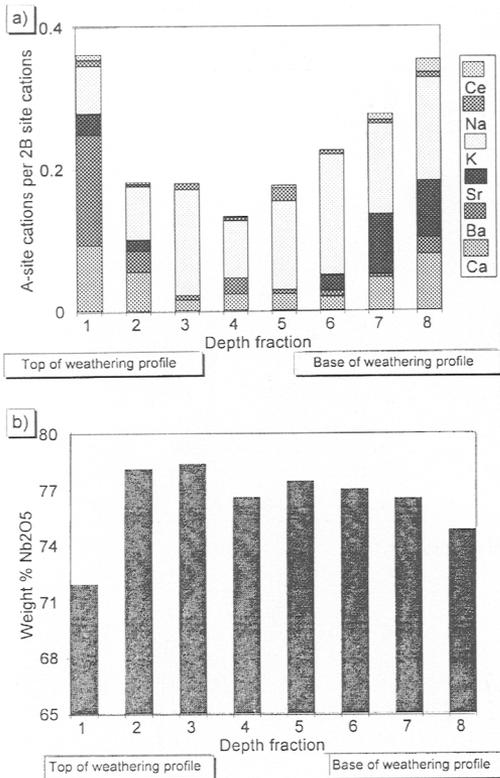
FIG. 6. An example of the variation in average pyrochlore composition with depth at Lueshe in one drill hole. Depth fractions are taken over about 3 m, each at about 3 m intervals (exact values not given for commercial reasons). (*a*) *A* cations; (*b*) Weight % Nb_2O_5.

1988), at Tomtor (Entin *et al.*, 1993), at Mabounié (Laval *et al.*, 1988) and in Siberian carbonatites (Lapin and Kulikova, 1989). Acid leaching experiments have been used to demonstrate the susceptibility of pyrochlore to this process (van der Veen, 1963; Lapin and Kulikova, 1989).

Kalipyrochlore, however, appears to be unique to Lueshe although there is some K-bearing pyrochlore reported from Russian carbonatites (Lapin and Kulikova, 1989) (Fig. 8). Also, apart from the initial cation leaching, neither pyrochlore from the weathered Mt Weld carbonatite (Lottermoser and England, 1988) nor pyrochlore from weathered Russian carbonatites (Lapin and Kulikova, 1989) show the same compositional trends with depth as Lueshe.

At Mt Weld, as at Lueshe, the compositional variation of the pyrochlore at any particular depth is large, there is little compositional zoning within the grains and the highest *A* cation deficiencies are in the centre of the profile (Lottermoser and England, 1988). In contrast with Lueshe, the general trend is one of progressive leaching of Ca and Na and their partial replacement by varying proportions of Sr and Ce rather than K, Ba and Sr.

Several (mostly un-named) weathered deposits overlying Russian carbonatites are discussed by Lapin *et al.* (1988), Lapin (1992) and Lapin and Kulikova (1989) and although no depth profiles are published, Ba, Ce and Sr pyrochlore are described as occurring throughout these lateritic deposits. At the Enisei Ridge (Lapin and Kulikova , 1989), bario-pyrochlore is reported to occur lower in the profile than strontiopyrochlore (in contrast to the pattern at Lueshe) but it is also suggested that the original mineralogy of the carbonatite determined the variety of pyrochlore that formed.

A sequence of progressive weathering without an accompanying spatial relationship is described by Entin *et al.* (1993). Fresh pyrochlore is divided into five types, predominantly Ca, Na pyrochlore, and this weathers to give successive generations of strontio-, Sr,Ba-, Ba,Sr- and then plumbopyrochlore. This sequence has some similarity to Lueshe in that in both cases Ba-rich pyrochlore occurs in highly weathered material.

Conclusions

1. The first and principal weathering reaction in Lueshe pyrochlore is hydration and leaching of *A* cations, together with partial uptake of new *A* cations. The alteration takes place early in the weathering process at the fresh rock interface and is common to pyrochlore in all weathered carbonatites so far reported worldwide.

2. The Lueshe deposit is unique in containing kalipyrochlore and the most likely reason for this is the abundance of K-feldspar in fresh carbonatite which weathers to release K. Initial rock composition is an important factor controlling the composition of weathered pyrochlore and can help to explain the wide range of chemical variation in pyrochlore generated through the weathering of various carbonatites.

3. Further variation in weathered pyrochlore at Lueshe was determined by several factors, including continued cation leaching, small variations in the initial Sr content of the primary, fresh pyrochlore, and further cation exchange and uptake.

4. The most important textural features of the pyrochlore are the intense fracturing of the grains and the intimate association with crandallite, which has nucleated around the pyrochlore grains, and in fractures and cavities within the grains.
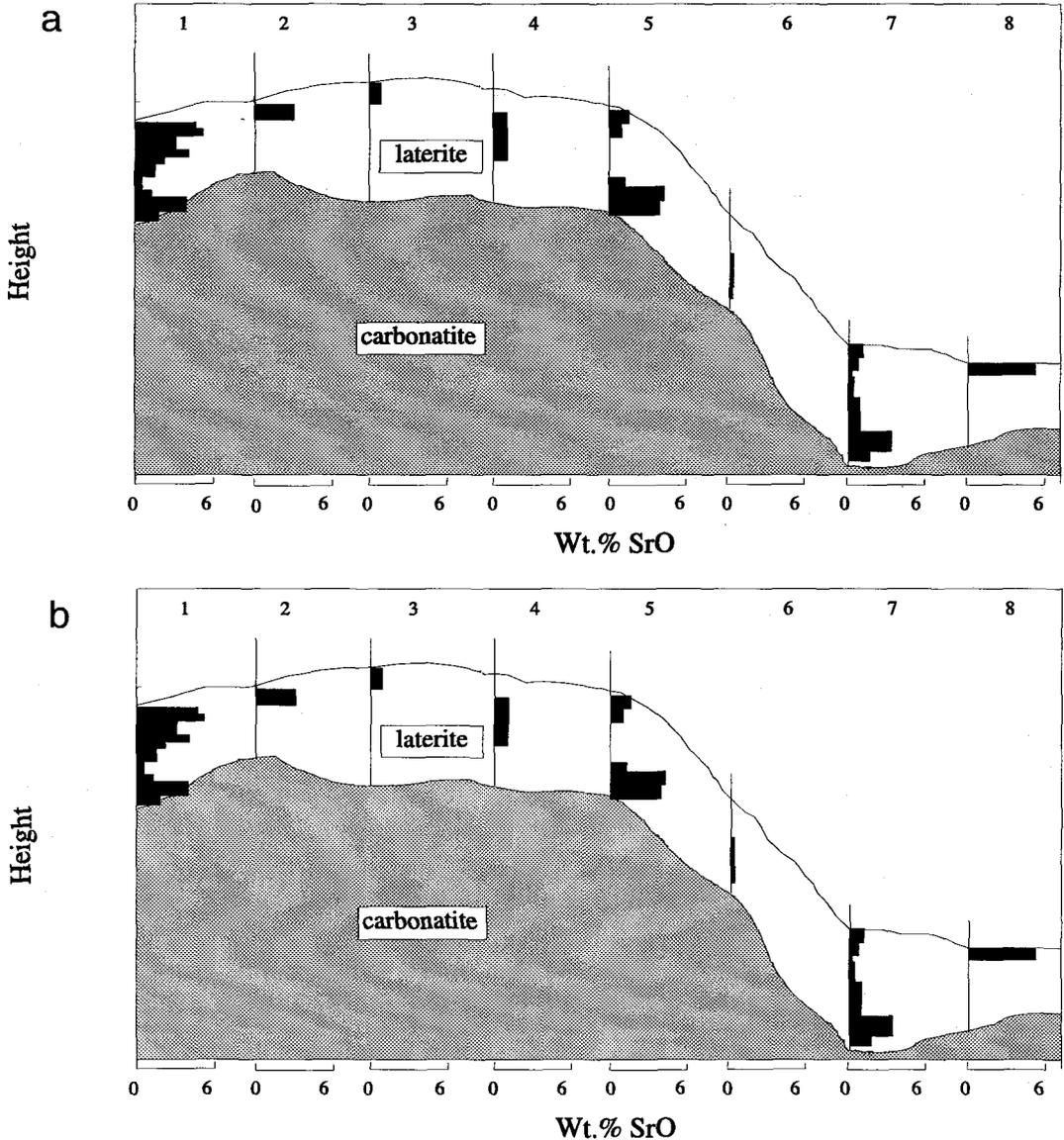
FIG. 7. (*a*) Logs of average pyrochlore composition in each depth fraction from 8 drill holes at Lueshe for Ba (*a*) and Sr (*b*). The position of the drill holes is schematic and the actual depth measurements are not shown, for commercial reasons. Not all drill holes extend through the complete profile.

5. The basic pyrochlore niobium-oxygen framework structure is highly resistant to weathering and persists throughout the weathering profile. Nb-bearing goethite found in a few samples of crandallitic ore probably represents the final mineral host for the Nb released by pyrochlore dissolution.
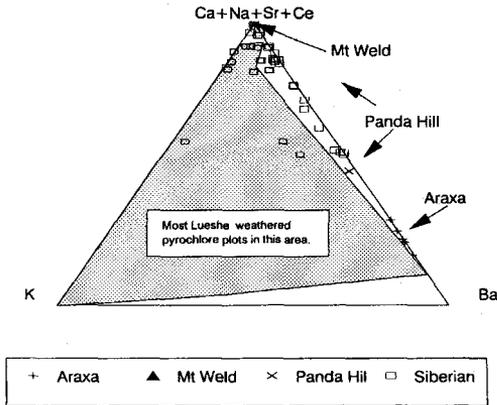
FIG. 8. Ternary diagram comparing, in terms of cations per formula unit, weathered pyrochlore from Lueshe with weathered pyrochlore from Mt. Weld (Lottermoser and England, 1988), Panda Hill (Jäger et al., 1959; Lumpkin and Ewing, 1995), Araxá (Issa Filho et al., 1984; Lumpkin and Ewing, 1995), and Siberian carbonatites (Lapin et al., 1989).

partners in the project at the Ecole des Mines, St. Etienne, France and the Université Catholique de Louvain, Belgium. Gary Jones prepared mineral concentrates of pyrochlore from the Lueshe fresh carbonatite and David Ratcliffe and Vicky Hards collected much valuable electron microprobe data during two vacation student projects. Don Hogarth, Gordon Cressey and an anonymous reviewer are thanked for their helpful comments which have much improved the manuscript.

References

Albers, K.-H., Alegria, B., Meixner, K.-T., Schuermann, B., Philippo, S., Naud, J., Verkaeren, J., Nasraoui, M., Bilal, E., Gracia, D., Gruffat, J.J., Guy, B., Moutte, J., Wall, F., Williams, C.T. and Woolley, A.R. (1994) *Applied mineralogy of pyrochlore and related minerals in the weathering zones of the niobium deposits of the Lueshe and the Bingo carbonatites, Zaire. Final Report to European Commission. EC Contract No: MA2M-CT90-0038.* Unpublished. 138 pp.

Bellon, H. and Pouclet, A. (1980) Datations K-Ar de quelques laves du Rift-ouest de l'Afrique Centrale: implications sur l'evolution magmatique et structurale. *Geologische Rundschau,* **69,** 49–62.

Clark, A.M. (1993) *Hey's Mineral Index.* Chapman and Hall, London. 852pp.

Chelishev, N.F. and Mar'ina N.A. (1972) The ion exchange properties of pyrochlore under super-critical conditions. *Doklady of the Academy of Sciences U.S.S.R. Earth Sciences Section,* **197,** 123–5. (Translated from O ionoobmennykh svoystvakh pirokhlora v nadkriticheskikh usloviyakh. *Doklady Akademii Nauk SSSR,* 1971, **197,** 682–5.)

Entin, A.R., Yeremenko, G.Y. and Tyan, O.A. (1993) Stages of alteration of primary pyrochlores. *Transactions (Dokaldy) of the U.S.S.R. Academy of Sciences: Earth Science Sections,* **320,** 1991, 236–9. (Translated from O stadiynosti izmeneniya pervichnykh pirokhlorov. *Doklady Akademii Nauk SSSR,* 1991, **319,** 1218–21.)

Ercit, T.S., Hawthorne, F.C. and Cern##, P. (1994) The structural chemistry of kalipyrochlore, a "hydropyrochlore". *Canad. Mineral.,* 32, 415–20.

Fleischer, M. and Mandarino, J.A. (1991) *Glossary of Mineral Species 1991.* The Mineralogical Record Inc, Tucson. 256 pp.

Hogarth, D.D. (1977) Classification and nomenclature of the pyrochlore group. *Amer. Mineral.,* **62,** 403–10.

Hogarth, D.D. (1989) Pyrochlore, apatite and amphibole: distinctive minerals in carbonatite. In *Carbonatites* (K. Bell ed.) Chapman and Hall, London. 105–48.

Issa Filho, A., Amorin dos Santos Lima, P.R. and Moreira de Souza, O. (1984) Aspects of the geology of the Barreiro Carbonatitic Complex, Araxá, MG, Brazil. In *Carbonatitic complexes of Brazil: geology.* CBMM, Department of Geology, São Paulo. 44 pp.

Jäger, E., Niggli, E. and van der Veen, A.H. (1959) A hydrated barium-strontium pyrochlore in a biotite rock from Panda Hill, Tanganyika. *Mineral. Mag.,* **32,** 10–25.

Jambor, J.L., Bladh, K.W. Ercit. T.S., Grice, J.D. and Grew, E.S. (1988) New mineral names. *Amer. Mineral.,* **73,** 927–35.

Lapin, A.V. (1992) Carbonatite Weathering Crusts: Geochemical Types and Mineralization. *Geochemistry International,* 29, 72–83.

Lapin, A.V. and I.M. Kulikova (1989) Alteration processes in pyrochlore and their products in weathering crusts of carbonatites. *Zapiski Vsesoyuznogo Mineralogicheskogo Obshchestva,* **118,** 41–49. (in Russian)

Lapin, A.V., Malyshev, A.A., Ploshko, V.V. and Cherepivskaya, G.Ye. (1988) Strontiopyrochlore from lateritic weathered mantle of carbonatite. *Transactions (Doklady) of the U.S.S.R. Academy of Sciences: Earth Science Sections,* 290, 188–192. (Translated from Strontsiopirokhlor iz lateritnykh kor vyvetrivaniya karbonatittov. *Doklady Akademii Nauk SSSR,* 1986, 290, 1212–7).

Laval, M., Johan, V. and Tourlière, B. (1988) La carbonatite de Mabounié: exemple de formation d'un gîte résiduel à pyrochlore. *Chron. Rech. Min.,* 491, 125–36.

Lottermoser, B.G. and B.M. England. (1988) Compositional variation in pyrochlores from the Mt Weld Carbonatite laterite, Western Australia. *Mineral. Petrol.,* **38**, 37—51.

Lumpkin, G.R. and Ewing, R.C. (1995) Geochemical alteration of pyrochlore group minerals: Pyrochlore subgroup. *Amer. Mineral.,* **80**, 732—43.

Maravic, H.v. and Morteani, G. (1980) Petrology and geochemistry of the carbonatite and syenite complex of Lueshe (N.E. Zaire). *Lithos,* **13**, 159—70.

Maravic, H.v., Morteani, G. and Roethe, G. (1989) The cancrinite-syenite/carbonatite complex of Lueshe, Kivu/NE-Zaire: petrographic and geochemical studies and its economic significance. *J. African Earth Sci.,* **9**, 341—55.

Meyer, A. (1958) La Carbonatite Lueshe (Kivu). *Congo Belge, 4e Direction Générale, Service Geologique,* Bulletin no. 8- Fasc. 5. 8 pp.

Nickel, E.H. and Nichols, M.C. (1991) *Mineral Reference Manual,* Von Nostrand Reinhold, New York. 250 pp.

van der Veen, A.H. (1963) *A study of pyrochlore.* Druk Van J.J. Groen & Zn. N.V., Leiden. 188 pp.

Van Wambeke, L. (1965) A study of some niobium-bearing minerals of the Lueshe carbonatite deposit (Kivu, Republic of Congo). *Report of European Atomic Energy Community — Euratom.* **EUR 2110.e.,** 1—30.

Van Wambeke, L. (1971) Pandaite, baddeleyite and associated minerals from the Bingo niobium deposit, Kivu, Democratic Republic of Congo. *Mineralium Deposita,* **6**, 153—5.

Van Wambeke, L. (1978) Kalipyrochlore, a new mineral of the pyrochlore group. *Amer. Mineral.,* **63**, 528—30.